Science of the Total Environment 658 (2019) 51–61

Contents lists available at ScienceDirect

Science of the Total Environment

journal homepage: www.elsevier.com/locate/scitotenv

Spatial characteristics and determinants of in-traffic black carbon in Shanghai, China: Combination of mobile monitoring and land use regression model

Min Liu [a,b,*], Xia Peng [c], Ziqi Meng [a], Taoye Zhou [d], Lingbo Long [a], Qiannan She [a]

[a] Shanghai Key Lab for Urban Ecological Processes and Eco-restoration, School of Ecological and Environmental Sciences, East China Normal University, Shanghai 200241, PR China
[b] Institute of Eco-Chongming (IEC), Shanghai 200062, PR China
[c] Library of East China Normal University, Shanghai 200241, PR China
[d] Pudong New Area Environmental Monitoring Station, Shanghai 200135, PR China

HIGHLIGHTS

- Mobile monitoring of in-traffic black carbon (BC) was conducted in Shanghai, China.
- BC was lowest in the urban core and increased towards the outer areas of the city.
- Land use regression (LUR) model could explain 68% of the BC spatial variability.
- The results implied the effect of traffic policy on the spatial BC in a Mega city.

GRAPHICAL ABSTRACT

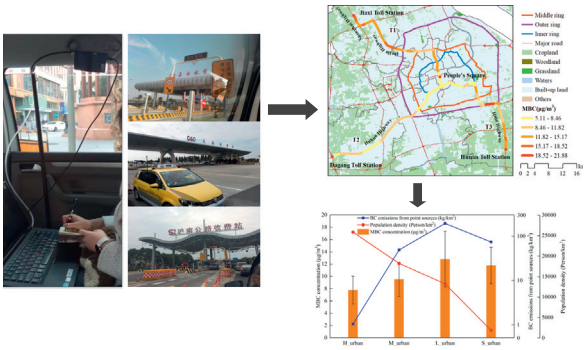

ARTICLE INFO

Article history:
Received 14 July 2018
Received in revised form 19 November 2018
Accepted 9 December 2018
Available online 13 December 2018

Editor: Pavlos Kassomenos

Keywords:
Black carbon (BC)
Mobile measurement
Urban environment
Land use regression model (LUR)
Shanghai

ABSTRACT

Black carbon (BC) has emerged as a major contributor to global climate change. Cities play an important role in global BC emission. The present study investigated the spatial pattern of in-traffic BC at a high spatial resolution in Shanghai, the commercial and financial center in Mainland China. The determinants including road network, social economic status and point-source pollutants, which may influence the BC spatial variability were also discussed. From October to December 2016, mobile monitoring was conducted to assess the BC concentrations on three sampling routes in Shanghai with a total length of 116 km. The results showed that the mean in-traffic BC among three sampling routes was 10.77 ± 3.50 μg/m^3. BC concentrations showed a significant spatial heterogeneity. The highest BC concentrations were near industrial sources and that those high concentrations were associated with either direct emissions from the industries, freight traffic, or both. With the widely distributed polluting enterprises and high emitting vehicles, the average BC in the low urbanization areas (12.80 ± 4.54 μg/m^3) was 57% higher than that in the urban core (7.77 ± 2.24 μg/m^3). Furthermore, a land use regression (LUR) model based on mobile monitoring was developed to examine the determinants and its spatial variability of BC measurements which corresponded to 17 predictor variables, e.g. road network, land use, meteorological condition etc., in 7 buffer distances (100 m to 10 km). The variables of meteorological, socio-economical and the distance to BC point-sources were selected as the independent variables. It was found that the established LUR

* Corresponding author at: Shanghai Key Laboratory for Urban Ecological Processes and Eco-Restoration, School of Ecological and Environmental Sciences, East China Normal University, Shanghai 200241, PR China.
E-mail address: mliu@re.ecnu.edu.cn (M. Liu).

https://doi.org/10.1016/j.scitotenv.2018.12.135

model could explain a proportion (68%) of the variability of BC. LUR modeling from mobile measurements was possible, but more work related to the effect of traffic regulation on BC could be helpful for informing best model practice.

1. Introduction

Black carbon (BC), which has been identified as the second largest contributor to global warming after carbon dioxide (CO_2) (IPCC, 2001, 2013), has important effects on climate change and human health (Booth and Bellouin, 2015). It is produced both naturally and by anthropogenic activities as a result of the incomplete combustion of fossil fuels, biofuel, and biomass and aggregates to particles with an aerodynamic diameter of 0.01–1.0 μm (Ramanathan and Carmichael, 2008). BC emissions originate from a variety of sources, including industrial (10%), residential (24%), mobile (24%), and open burning (42%) (Ni et al., 2014). However, BC sources vary by region and time depending on life-style and the types of fuel used. Meanwhile, as important components of fine particulate matter (PM), BC can penetrate deeply into respiratory systems and cause respiratory and cardiovascular diseases and mortality (Geng et al., 2013; Dabass et al., 2016). Furthermore, BC stays in the atmosphere for only several days to weeks (i.e. 4–12 days) (Cape et al., 2012). Controlling BC emissions could have immediate cooling effect on the earth's climate with co-benefit of air quality (Hansen et al., 2000; Grieshop et al., 2009).

Precise measurements of atmospheric BC concentrations are indispensable for understanding BC source origin and environments effects. The earliest systematic measurements of BC started in London towards the end of 19th century (Harrison, 2006). Since 1980s, BC has been included in the observation program of Global Atmosphere Watch (GAM) by World Meteorological Organization (WMO). Moreover, the interest of policy makers in BC was aroused due to emerging evidence on health effects and the impact of BC on global warming. More recent records in related research have also been made in Antarctica (Hansen et al., 2001), the United States (Vilcassim et al., 2014; Kirchstetter et al., 2017), India (Safai et al., 2013; Begam et al., 2016), Switzerland (Liu et al., 2010), South Africa (Moloi et al., 2002), and Italy (Invernizzi et al., 2011). These researches mainly focused on the BC radiative impact and optical property (Menon et al., 2002; Dumka et al., 2013; Tan et al., 2016), spatial and temporal characteristics (Qin and Xie, 2012; Safai et al., 2013), source apportionment (Rajesh and Ramachandran, 2017) and health effects (Janssen et al., 2011). In developed countries, motorized transport (mainly diesel vehicles) are considered to be the most important source of BC in cities, whereas in developing countries biomass burning may be more remarkable (Highwood and Kinnersley, 2006; Kirchstetter et al., 2008).

Cities account for ~70% anthropogenic greenhouse-gas emissions (Grimm et al., 2008; Nordbo et al., 2012) and have suffered from poor air quality (Chan and Yao, 2008; Ding et al., 2016). Traffic exhaust emission is the main source of BC in urban areas, which has a significant impact on atmospheric BC concentration (Kim et al., 2017; Winiger et al., 2017). Understanding and quantifying the BC concentration in cities could offer a powerful lens into urban systems and provide a compact metric of urban sustainability (Latha and Badarinath, 2004; Zhang et al., 2015). Extensive development of BC measurements in urban environments of New York (Rattigan et al., 2013), Pune (Safai et al., 2013) and Paris (Laborde et al., 2013) has been carryout recently (Rattigan et al., 2013; Zhang et al., 2015). Most of these studies were based on continuous observations in common-point measurements, and the general conclusions were that urban BC concentrations showed obvious daily, weekly and seasonal variation, which was mainly influenced by traffic condition (Targino et al., 2016), vehicle type (Kim et al., 2017) and biomass burning (Safai et al., 2013). However, traditional stationary monitoring stations were unable to acquire BC measurements at a high spatial resolution. Due to the great heterogeneity of emission sources in urban area, atmospheric BC concentration showed large differences in space and time on a small scale (Van den Bossche et al., 2015). Recently, mobile monitoring in the application of air pollutant measurement are increasingly being accepted, especially for traffic-related pollutions, e.g. BC, NO_2, NO and PM (Hankey and Marshall, 2015a; Dekoninck et al., 2015; Morales Betancourt et al., 2017). The land use regression (LUR) model, an assessment tools in air pollution epidemiological researches, evaluates the relationship between observed air pollution concentrations and predictor variables (e.g. land use and traffic condition) in the multivariate regression model (Dons et al., 2013). LUR modeling with mobile measurements is practicable reported by Hankey and Marshall (2015b). However, only few studies used mobile measurements as a basis for LUR modeling (Van den Bossche et al., 2018).

Shanghai, located in southeastern China, is one of the most densely populated city in the world with significant air quality issues. Precise estimation for the spatial distribution of atmospheric in-traffic BC could promote the developments of pollutant emission control and epidemiologic study. In this study, the results of in-traffic BC made in Shanghai are presented. The primary goals of present research were (1) to provide the spatial variability of in-traffic BC in urban environment with a high spatial resolution, (2) to investigate how BC is dependent on urban gradients, traffic conditions, meteorological parameters and other sources, and (3) to develop LUR models for predicting spatial patterns in BC for Shanghai.

2. Methodology

2.1. Study area

Shanghai (30°40′–31°53′N, 120°52′–122°12′E, Fig. 1), located on the eastern coast of China, is a global financial center and the most populous city in the world. It has a population of 24.19 million in 2016, covers an area of 6340 km^2. The region has a humid subtropical climate and experiences four distinct seasons, with an average temperature of 17.7 °C and receives 1222.2 mm/year of precipitation during the past 15 years. As the financial and commercial center of mainland China, its gross domestic product (GDP) reached CNY 2.74 trillion (USD 397.11 billion) in 2016, accounting for 3.68% of the national GDP (Shanghai Municipal Statistics Bureau, 2017). The tertiary industry, mainly including financial services, retail and real estate, provides 70.13% of the total output. Shanghai is well developed in transportation, with the railway, road and inland waterway covering distance of 456, 13,195, and 2059 km, respectively. The number of vehicles increased from 1.39 to 3.59 million during 2002–2016. Its rapid energy consumption growth and high degree of urbanization has resulted in a remarkable increase of air pollutant emissions.

Based on the officially issued document “The overall urban planning of Shanghai (Year 1999–2020)”, Shanghai is classified into four different urbanization gradients according to the three ring roads: the high-degree urbanization (H_urban, within the Inner Ring Road), the moderate-degree urbanization (M_urban, outside the Inner Ring Road and within the Middle Ring Road), the low-degree urbanization (L_urban, outside the Middle Ring Road and within the Outer Ring Road) and suburban (S_urban, outside the Outer Ring Road) (Fig. 1).

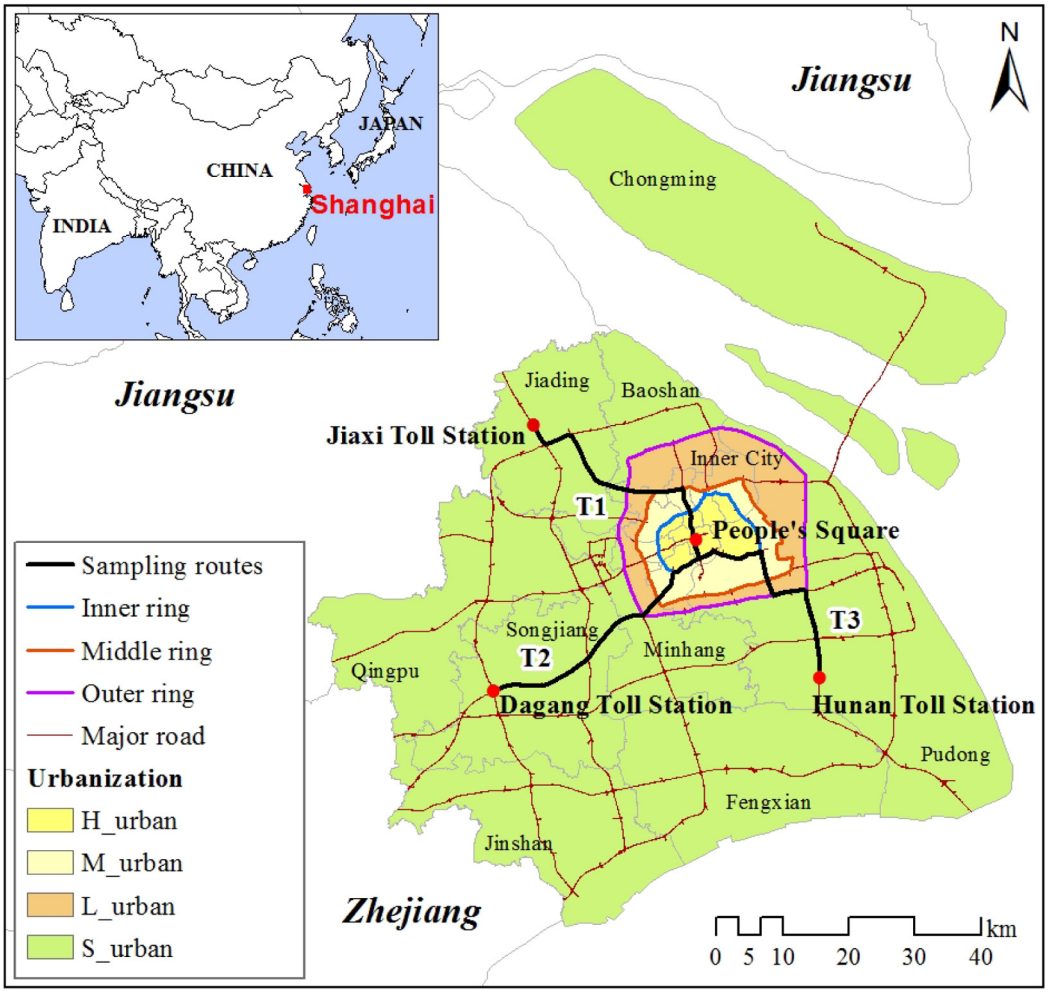

Fig. 1. Map of the study area in Shanghai with three sampling routes. The Inner City mainly consists of Huangpu, Jing'an, Hongkou, Yangpu, Xuhui, Changning and Putuo district.

2.2. Field mobile measurements of BC concentrations

The in-traffic BC concentrations in the urban districts along three designated sampling routes was measured in this study using fossil fuel based car as mobile sampling platform. These three sampling routes all started at People's Square, and ended at Jiaxi Toll station (T1, northwest), Dagang Toll station (T2, southwest) and Hunan Toll station (T3, southeast), respectively (Figs. 1 and 2). These sampling routes passed the city expressways within the Outer Ring Road and the highways outside the Outer Ring Road, with different urbanization gradients, road configurations and traffic densities. The sampling campaigns were conducted during weekday mornings (09:00–11:00 am) on rainless days in October and December 2016, with clear skies and calm winds to avoid misrepresentation of typical urban air pollution conditions. To minimize the influence of inconsistency in time and external environment on BC sampling, round trip and triplicate measuring were made for each sampling route. To be specific, there were 3 runs per route for the entire campaign. The detailed description for each sampling runs was illustrated in Table 1, including the sampling date, meteorological conditions and the corresponding route. To obtain a representative and reliable picture of BC in urban area, three round-trip measurements was carried out to minimize the uncertainty caused by the discrepancy in time and abnormal conditions (i.e. traffic jam and nearby traffic). In total, nine sampling runs (~348 km of on-road measurements) were completed among the sampling routes (~116 km).

A portable aethalometer (AE51, AethLabs, USA) was used to measure the BC concentrations in traffic environment. The microaethalometer determined the BC concentrations by measuring the attenuation of an 880 nm radiation beam transmitted through a filter strip. The instrument had its own sampling inlet with a Bev-A-line tubing, equipped in the middle of the vehicle with 2 m above ground level (Fig. 2). According the World Meteorological Organization (WMO), all aerosol measurements should to be made at a relative humidity below 40% for best accuracy (WMO/GAW, 2003). As relative humidity was quite high in Shanghai, an aerosol stream dryer (Magee Scientific) was used to remove water vapor from the sample stream by diffusion through Nafion membrane during each sampling campaign. Meanwhile, a GPS device (Juno SB, Trimble) recorded the spatial coordinates of all sampling at the time of data collection, with the temporal resolution the same as the BC analyzer (10 s). The average travel speed during the sampling campaign was about 40–50 km/h (i.e. 11.1–13.8 m/s) and BC measurements recorded at 10 s time interval, about 120 m apart. The instruments were prepared in the laboratory before each sampling campaign, consist of changing of the AE51 filter strip, zero calibration, battery and memory checks.

The aethalometer frequently recorded spurious concentration "spikes" when exposed to mild mechanical shock or vibration (Apte et al., 2011). In addition, the measurements could be heavily impacted by nearby traffic. Therefore, we recorded the standing time of traffic lights or traffic jams during sampling, such as the location, starting time and duration. When the distance between two adjacent BC

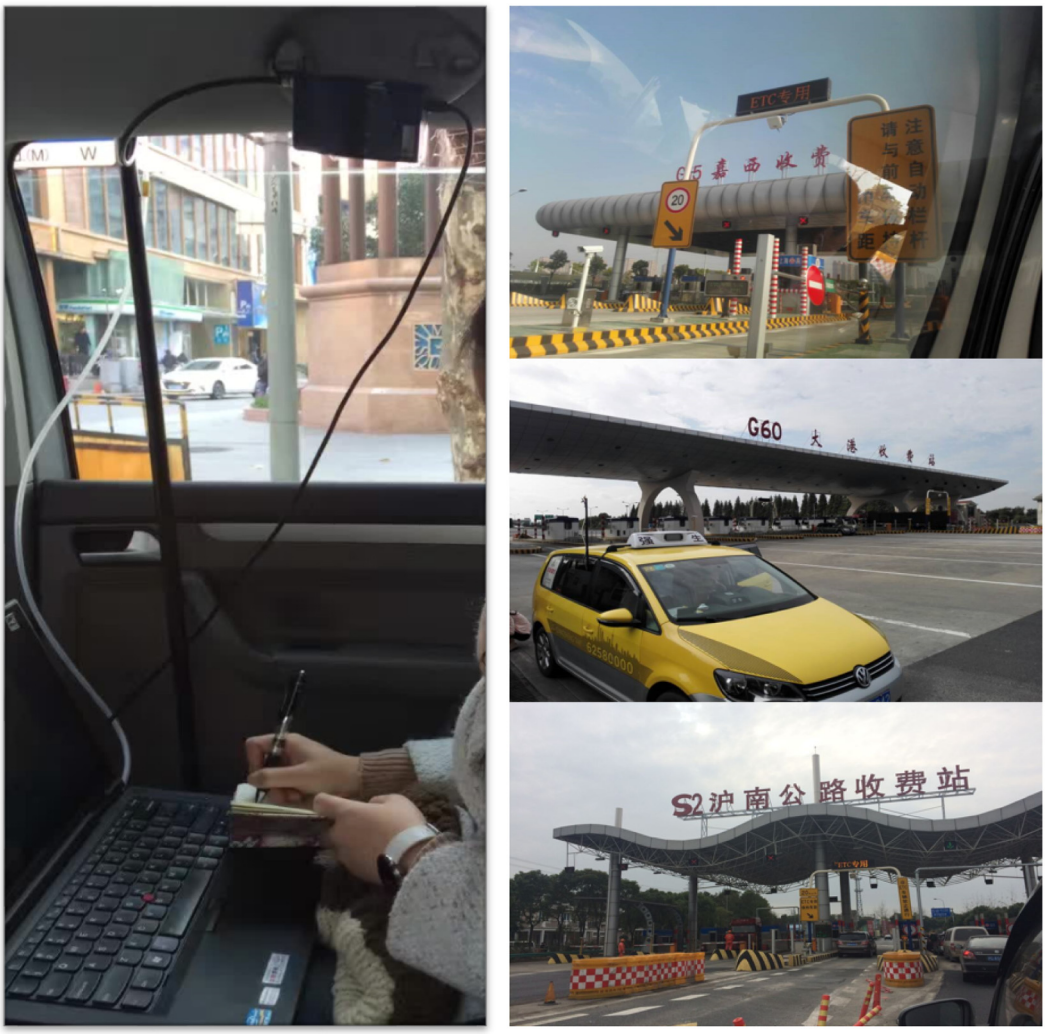

Fig. 2. Mobile sampling platform and three destinations of the three sampling routes. The three pictures on the right are Jiaxi Toll station, Dagang Toll station and Hunan Toll station in sequence from top to bottom.

sampling points was <55 m (i.e. 20 km/h, the average speed during traffic jams in expressways), the second BC record was regarded as "spikes". After spike screening, the valid BC measurements were 88.4% of the total observations with 10 s interval. Moreover, to reduce the impact of negative value on BC exposure concentrations, the Optimized Noise-reduction Averaging (ONA) algorithm described in Hagler et al. (2011) and Cheng and Lin (2013) was adopted. K-N corrections developed by Kirchstetter and Novakov (2007) were applied to BC exposure measurements to correct for underestimations of BC concentrations with increasing aethalometer filter loading (Kirchstetter and Novakov, 2007; Hagler et al., 2011). The following equations were used to compensate the filter loading effect of BC concentrations:

$$BC = \frac{BC_0}{(0.88Tr + 0.12)} \quad (1)$$

$$Tr = \exp(-ATN/100) \quad (2)$$

where BC was the corrected BC, BC_0 was the observation data, T_r was the aethalometer filter transmission, which was calculated from the

Table 1
Descriptions of the meteorological conditions during the sampling campaigns.

Date	Transect	Air temperature (°C)	Relative humidity (%)	Wind speed (m/s)	Wind direction
Oct. 18	T2	21.58	79.14	1.74	NE
Nov. 4	T1	15.51	77.15	1.33	NS
Nov. 30	T3	11.13	75.81	1.47	NW
Dec. 2	T2	9.06	75.83	1.07	NE
Dec. 6	T3	7.94	68.58	1.15	NE
Dec. 7	T1	10.06	71.58	0.96	S
Dec. 8	T3	10.90	71.10	1.31	S
Dec. 9	T2	10.55	69.52	2.11	N
Dec. 15	T1	3.86	57.03	2.24	NW

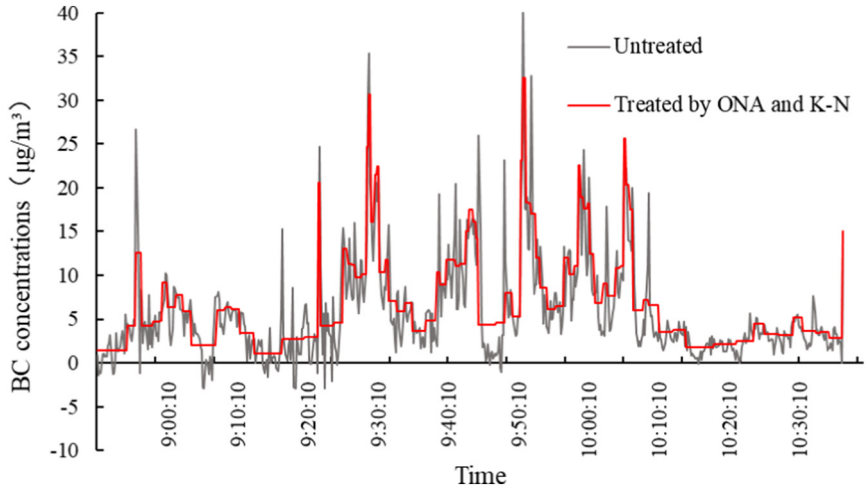

Fig. 3. The comparison between original BC measurements and corrections treated by ONA and K-N was illustrated in this figure (take T3 monitored on December 6 for example).

measurements of transmitted light intensity (ATN). The comparison between original BC measurements and corrections treated by ONA and K-N was illustrated in Fig. 3 (take T3 monitored on December 6 for example).

2.3. Spatial and socioeconomic variables

To investigate the potential effects of natural condition and human activities on the spatial distribution of in-traffic BC concentrations, 17 variables in 7 buffer distances (100 m, 500 m, 1 km, 2.5 km, 5 km, 7 km and 10 km) were tested for their associations to the observed BC concentrations in traffic environment over Shanghai. The variables were grouped into six categories: (1) road network (length of major and minor roads and distance to major and minor roads); (2) land use (areas of cropland, woodland, grassland, waters and built-up land); (3) meteorology (wind speed, relative humidity, temperature and atmospheric boundary layer height); (4) socio-economy (population density and gross primary production); (5) physical geography (elevation); and (6) point-source pollutant (distance to BC point-source pollutant) (Table 2).

As it was very difficult to acquire the vehicle population (i.e. high emitting vehicles, relative clean vehicles), the road variables were used to reflect the traffic information. The road data for the study area was obtained from the OpenStreetMap (Mooney et al., 2016), including urban expressways, highways, national roads, provincial roads, county roads and rural roads. Considering the traffic flow/intensity, we divided the roads into two types, i.e. major road (urban expressways and highways) and minor road (other four types of roads). The land use/cover data with a spatial resolution of 30 m were provided by the National Geomatics Centre of China (NGCC). Pixel-object-knowledge based approach was implemented on images from Landsat Thematic Mapper (TM), Enhanced Thematic Mapper plus (ETM+), and the HJ-1 (multispectral images of Chinese Environmental Disaster Alleviation Satellite), with a high accuracy of over 80% (Chen et al., 2015). As the meteorological conditions with the mobile sampling platform were not recorded in this study, the hourly weather variables (wind speed-WS, relative humidity-RH, and temperature-T) were obtained from 11 meteorological stations in Shanghai, provided by the National Climate Center of the China Meteorological Administration (CMA). Inverse Distance Weighted (IDW) interpolation algorithm provided in Arcgis 10.3 was used to create the spatial distribution map of each weather variables.

Table 2
Descriptions of potential predictor variables on spatial variation of BC exposure concentration.

Categories	Variables/units	Description	Data sources
Road	Len_MajorRoad (m) DIST_MajorRoad (m) Len_MinorRoad (m) DIST_MinorRoad (m)	Total length (LEN) of major and minor road, average distance (DIST) to major and minor road in 7 buffer distances	Shanghai Key Lab for Urban Ecological Processes and Eco-Restoration
Land use	Area_Cropland (m^2) Area_Woodland (m^2) Area_Grassland (m^2) Area_Waters (m^2) Area_Build-upland (m^2)	Total area of cropland, woodland, grassland, waters and built-up land in 7 buffer distances	Globeland30-2010 (http://www.globalland-cover.com)
Meteorology	WS (m/s) RH (%) T (°C) BLH (m)	The average value of wind speed (WS), Relative Humidity (RH), Temperature (T) and atmospheric boundary layer height (BLH) in 7 buffer distances	Chinese Meteorological Administration (http://data.cma.cn/data/) The European Centre for Medium-Range Weather Forecasts (ECMWF) (http://apps.ecmwf.int/datasets/data/interim-full-daily/levtype=sfc/)
Socio-economy	POP (person) GDP (RMB ten thousand yuan)	The average value of population (POP) and gross domestic product (GDP) in 7 buffer distances	WorldPop datasets (http://www.worldpop.org.uk/data/get_data/) Global Change Research Data Publishing & Repository http://geodoi.ac.cn/WebCn/CategoryList.aspx?categoryID=9
Physical geography	DEM (m)	Average of elevation (DEM) in 7 buffer distances	SRTM 90 m Digital Elevation Data (http://srtm.csi.cgiar.org/)
Point-source pollutant	DIST_PSP (m)	Average distance (DIST) to BC point-source pollutant (PSP) in 7 buffer distances	BC point-source distribution in Shanghai supported by Pudong New Area Environmental Monitoring Station, Shanghai

Afterwards, a summary measure for the 2-hour sampling period for WS, RH and T was obtained. Weather and air quality are also related to dynamic variations of planetary boundary layer processes (Vinogradova et al., 2007; Leventidou et al., 2013). In this study, the daytime BLH during the study period was downloaded from the European Centre for Medium-Range Weather Forecasts, which was available at a 0.125° × 0.125° latitude-longitude resolution.

In addition, the population data in Shanghai was obtained from WorldPop datasets, where population numbers per 100 × 100 m grid square are estimated. Meanwhile, the gridded GDP map was provided by Global Change Research Data Publishing & Repository. The elevation for the study area was obtained from The NASA Shuttle Radar Topographic Mission (SRTM) with a spatial resolution of 90 m × 90 m. The distribution and emissions of polluting enterprises was provided by the Shanghai Environmental Protection Bureau.

To further explore the relationship between spatial patterns of BC concentrations and potential influencing factors, we divided three sampling routes into 116 segments (1 km each). BC measurements along 1 km segments (~8 data points) were aggregated to ensure that aggregation location could provide sufficient sample sizes to estimated concentrations. As the distance between aggregation locations decreases, the number of measurements per location decreases. After that, we created the line buffer around each entire segment and the statistical average values of predictor variables in different buffer sizes around each segment were calculated.

To avoid the dimension problem caused by different types of data in subsequent analysis, all potential predictor variables were standardized using the Z-Score method. The Z-scores were computed for all the independent variables:

$$z = \frac{x-\mu}{\sigma} \tag{3}$$

where z is standardized variate, also called the z-score, following a normal distribution with zero mean and one variance. μ and σ indicate the mean and variance of x. Seventeen variables in 7 buffer, in total 119 (17 × 7) spatial predictor variables, were all considered in LUR model development. ArcGIS and SPSS were used to evaluate, modify, extract, and aggregate potential predictor variables.

2.4. BC modeling with land use regression model

Land use regression (LUR) is a statistical technique used to determine exposure to air pollutants in epidemiological studies (Dons et al., 2013). It is a cost-effective tool for predicting spatial variability in ambient air pollutant concentrations with high resolution (Hankey and Marshall, 2015b). Traditionally, in a LUR model, air pollutants measured at 20–100 monitoring stations was used as the dependent variable entered in a multiple linear regression analysis with several geospatial variables (e.g. traffic, land use or population density) as independent variables (Dons et al., 2013; Montagne et al., 2015). LUR models have been developed for $PM_{2.5}$, NO_2, and BC in many cities (Saraswat et al., 2013; Nunen et al., 2017). However, LUR model developed by pollutant concentrations based on mobile measurements is likely to be relatively limited (Hankey and Marshall, 2015a, 2015b; Van den Bossche et al., 2018). On condition of the limited funds, mobile monitoring not only expands spatial coverage for data acquisition, but also enlarges the sample size for LUR model (Van den Bossche et al., 2015).

In this study, we developed LUR models using mobile BC measurements in traffic environment. The natural logarithm of the median BC concentration (lnMBC) on per segment (1 km) was used as the dependent variable in a multiple linear regression analysis (Hankey and Marshall, 2015a), with a total of 116 data records. The main procedures for developing LUR model in this study included: (1) conducting bivariate analysis to find the significant independent variables that explained the dependent variable of lnMBC. Variables kept had to be significant at the 95% level ($p < 0.05$); (2) selecting the variable with the highest correlation coefficient in 7 buffer distances; (3) excluding the variables of high collinearity with other variables (variance inflation factor [VIF] >3); and (4) developing the stepwise regression model with the selected independent variables. All these processes were completed in SPSS.

The final models were evaluated with the leave-one-out cross validation method (LOOCV). To explore the global and local patterns of spatial autocorrelation for the LUR model to BC, the model residuals were analyzed by calculating Moran's I statistic and the Anselin local Maran's

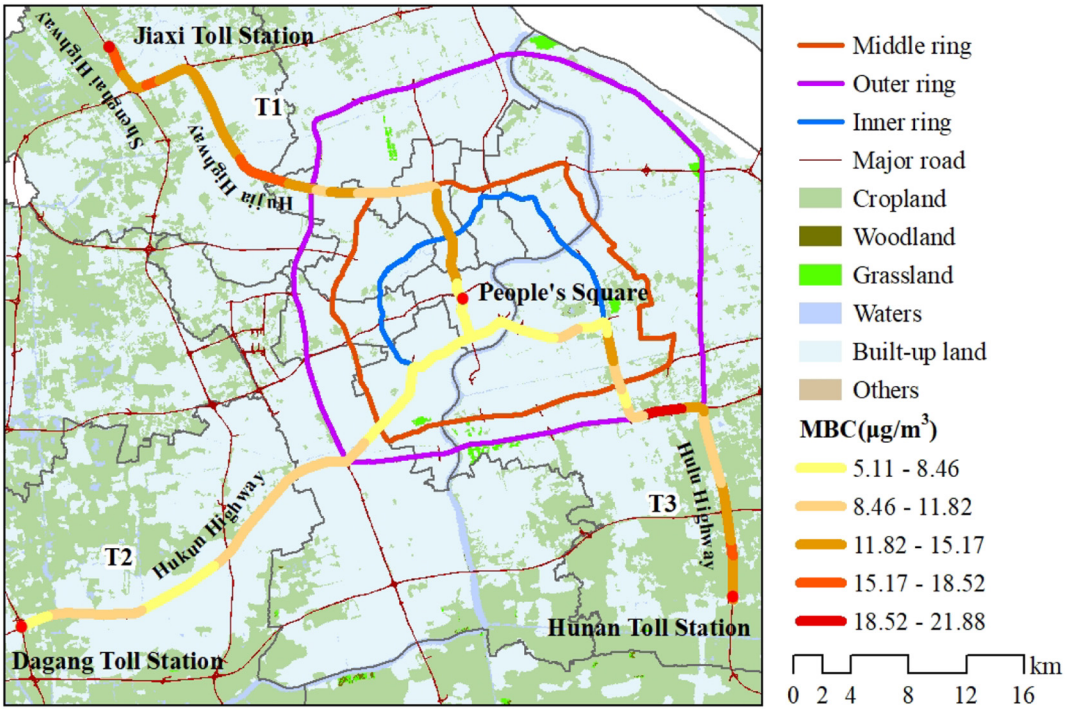

Fig. 4. Spatial distribution of the median BC (MBC) exposure concentrations at 1 km segment of three sampling routes in Shanghai.

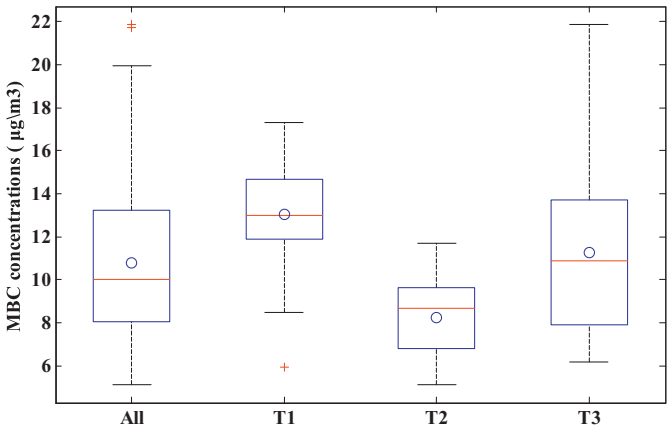

Fig. 5. Boxplot of median BC concentrations for three sampling routes. Black horizontal bars correspond to the lower and upper quartile values. The red lines and blue dot showed the median and means, respectively. (For interpretation of the references to color in this figure legend, the reader is referred to the web version of this article.)

I (LISA). In addition, we mapped BC concentrations at a 100 m of spatial resolution by rendering the regression models in ArcGIS.

3. Results and discussion

3.1. Spatial variations of BC concentrations across urbanization gradients

The median BC (MBC) concentration per segment (1 km) was showed in Fig. 4. The observed MBC concentrations in traffic environment exhibited substantial spatial heterogeneity, with the lowest value in the urban core and the highest in the northwest and southeast parts. The MBC of all three sampling routes in traffic during 09:00–11:00 am varied from 5.11 μg/m^3 to 21.88 μg/m^3, with an average value of 10.77 ± 3.50 μg/m^3 (Fig. 5). Among three sampling routes, the average of MBC in T1 (13.05 ± 2.54 μg/m^3) was obviously higher than those of T2 (8.23 ± 1.74 μg/m^3) and T3 (11.26 ± 3.96 μg/m^3). The areas with high traffic intensities, particularly on the highways, showed the high MBC concentrations (Fig. 4), e.g. the Hujia Highway and the Shenhai Highway in T1 (12.3 ± 0.8 μg/m^3), the Hulu Highway in T3 (11.0 ± 1.6 μg/m^3) and the Hukun Highway in T2 (8.7 ± 1.4 μg/m^3). In addition to the MBC on highway, the high values appeared in T1 and T3 were around the Outer ring road.

Compared to other studies in traffic environments in Shanghai, the mean of MBC concentrations observed in this study was higher than the result in Li et al. (2015) (8.62 ± 4.13 μg/m^3), but lower than that reported by Lei et al. (2017) (11.8 ± 9.8 μg/m^3) on three ring roads with mobile monitoring during October 2015 in Shanghai. This discrepancy could be partly attribute to the different sampling routes in these three studies. In general, the in-traffic BC of Shanghai was relatively higher than that observed in cities of other countries. For example, a study in Londrina (Brazil) based on bicycle sampling found that the average BC concentration was 6.4 ± 20.0 μg/m^3 (Targino et al., 2016). According to Hankey and Marshall (2015a, 2015b), the measurements of on-bicycle exposure to BC, between August 14 and October 16, 2012 in Minneapolis, were 2.5 ± 1.4 μg/m^3 in the morning and 0.7 ± 1.6 μg/m^3 in the afternoon. Although the mobile platforms and sampling instruments were not consistent in different cities, the high BC measurements in Shanghai could partly reflect a strong pressure of air pollution and human health compared to the cities in other countries around the world.

Based on the classification of urbanization levels in Shanghai, the average MBC concentrations of H_urban, M_urban, L_urban and S_urban in Shanghai were 7.77 ± 2.24, 9.51 ± 2.76, 12.80 ± 4.54 and 11.77 ± 2.94 μg/m^3, respectively (Fig. 6). Correspondingly, the population density in the H_urban areas of Shanghai was 25,838 person/km^2, which was two folds and 13 folds than that in the L_urban areas (13,225.85 person/km^2) and S_urban areas (1880.26 person/km^2). In general, cities density is strongly correlated with concentrations of greenhouse gases, especially for CO_2 and CH_4; however, it does not appear to be so in this study. There was a clear rise of BC concentrations in L_urban areas compared to that in H_urban and M_urban areas, with the exception that MBC in S_urban was slightly higher than that in M_urban.

Further analysis indicated that the variation of BC concentrations levels among urbanization gradients in Shanghai were consistent with the BC emissions that omitted from industrial and power sectors. According to the information provided from Shanghai Environmental Protection Bureau in 2015, >95% of polluting enterprises were located outside the Outer Ring road. The BC emissions from these polluting enterprises were about four-fold in L_Urban (195.33 kg/km^2) than that in M_urban (49.14 kg/km^2). These industrial sources lead to the highest BC concentrations appeared in the low density areas. In the suburban areas outside the outer ring, due to the reduction of BC industrial source emissions, the BC concentration has also declined. We could conclude that the direct emissions from the industries could be an important BC sources in Shanghai.

On the other hand, the container cars and diesel-fueled heavy trucks were banned on the Inner and Middle Ring roads in Shanghai since October 2016. This stop-and-go traffic may lead to larger BC emissions in low-urban and suburban areas compared to that in the high and median density areas within Middle Ring road. We could inferred that it may be the combustion conditions of the vehicles and not the volume that have

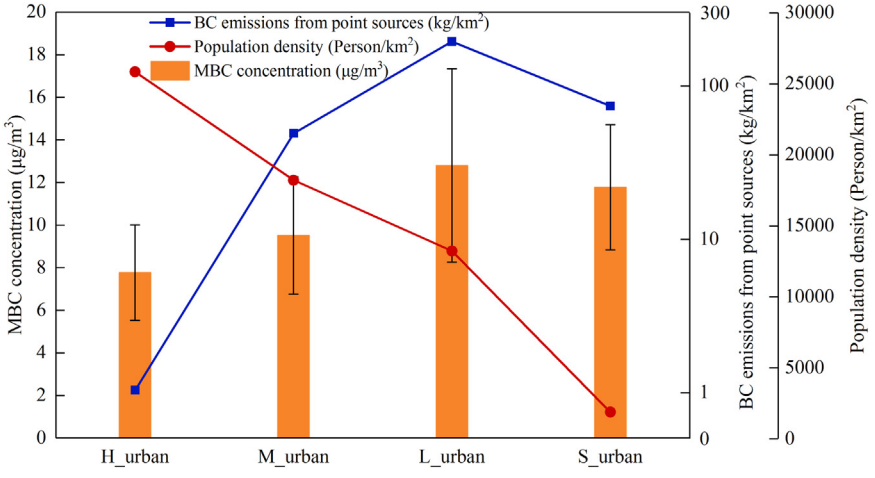

Fig. 6. MBC exposure concentrations, population density and BC emissions from point sources in different urbanization levels.

significant effect on the regional BC concentrations in Shanghai. Different vehicle population (i.e. high emitting vehicles, relative clean vehicles) could contribute to the different BC concentration at different area. Targino et al. (2016) pointed out that older buses and diesel-powered trucks may be the main driver behind the high pollution levels in the city's inner core. Wang et al. (2011) also found that 5% of diesel trucks were responsible for 50% of total BC emissions, and 20% of the trucks were responsible for over 70% of BC emissions in Beijing, China. A number of studies also found that diesel truck emission regulations, including combustion conditions of the engines and malfunctioning emission control systems could lead to the declining BC concentrations (Bahadur et al., 2011; Murphy et al., 2011). However, the high flow of high-pollution trucks combined with the straw burning activities in rural areas could result in higher levels of MBC concentrations.

In summary, the highest BC concentrations in Shanghai were near industrial sources in the low density areas and that those high concentrations appeared in L_urban and S_urban were associated with either direct emissions from the industries, associated freight traffic, or both. These reasons for the BC variations among different urban gradients were in accordance with the findings in Kirchstetter et al. (2017), in which large reductions in urban BC concentrations was found between 1965 and 2000 across U.S., contrast increasing energy use and CO_2 emissions. The substituting natural gas and electricity for heavy fuel oil and decreasing emissions from diesel vehicles contributed to the significant decline of BC concentrations.

3.2. Association of BC concentrations and potential influencing factors

The Pearson correlation coefficient (r) between MBC concentrations and independent variables was calculated within a certain spatial scale of different buffer distances. The results indicated that MBC concentrations were significantly correlated with 73 of the 119 variables under 7 buffer distances (Fig. 7). The result showed that the spatial distribution of MBC was more influenced by variables of meteorology, socio-economy, physical geography and point-source pollutants than that of road and land use. In terms of absolute value, the correlation coefficients (r) between MBC concentrations and WS, RH and T were mostly above 0.45, especially the largest value ($r = 0.75$) occurred in WS.100 m (the average wind speed in 100 m buffer distance). For road and land use variables, their influences on MBC mainly occurred within the range of between 100 m and 2.5 km, while GDP and POP showed stronger correlations with MBC in larger buffer distance, particularly GDP.5 km (the average GDP in 5 km buffer distance). The remaining DEM and DIST_PSP both had significant effects ($p < 0.01$) on MBC in all buffer distances, and r of DEM was higher than DIST_ PSP.

It was worth noting that correlation coefficients (r) between some variables and MBC appeared as unusual positive and negative signs, such as the length of roads (negative), the distance to roads (positive), the areas of built-up land (negative), wind speed (positive), boundary layer height (positive) and populations (negative). It couldn't assert that these relationships were wrong as mobile monitoring, different from station measurements, was inescapability affected by the ever-changing traffic environment (Dons et al., 2013), including vehicle populations and near-surface meteorological conditions. As different vehicle population contributes to the BC concentration at different area, we may infer that, the population of high emitting vehicles was larger in the areas with high road network density than that areas with low road network density in Shanghai. Nevertheless, except for some variables which were not sure about the positive or negative relationship (e.g. DEM and temperature), remaining variables showed popular signs, for example the higher GDP or the less distances to BC point sources will result in higher MBC concentrations.

3.3. Evaluation and prediction of BC concentrations with LUR model

By combining MBC observations and the possible independent variables, we were able to develop a predictive LUR models for the spatial distribution of BC in traffic environment in Shanghai. Specifically, four variables were selected to describe the predicted spatial distribution of BC exposure in LUR modeling in this study, which included WS.100 m, RH.100 m, GDP.5 km and DIST_PSP.1 km (Table 3). It was important to note that the road variables failed to the variable screening. This result illustrated that the effects of road distribution and land use on BC concentrations were relatively small in LUR modeling compared to meteorological variables.

For the model performance, the established LUR model in this study could explain a proportion (68%) of the variability in measured BC concentration, with an adjusted R^2 of 0.67 and an LOOCV R^2 of 66%. Compared to LUR models developed in other study areas, the result of our study might show a higher adjusted R^2. For example, Montagne et al.

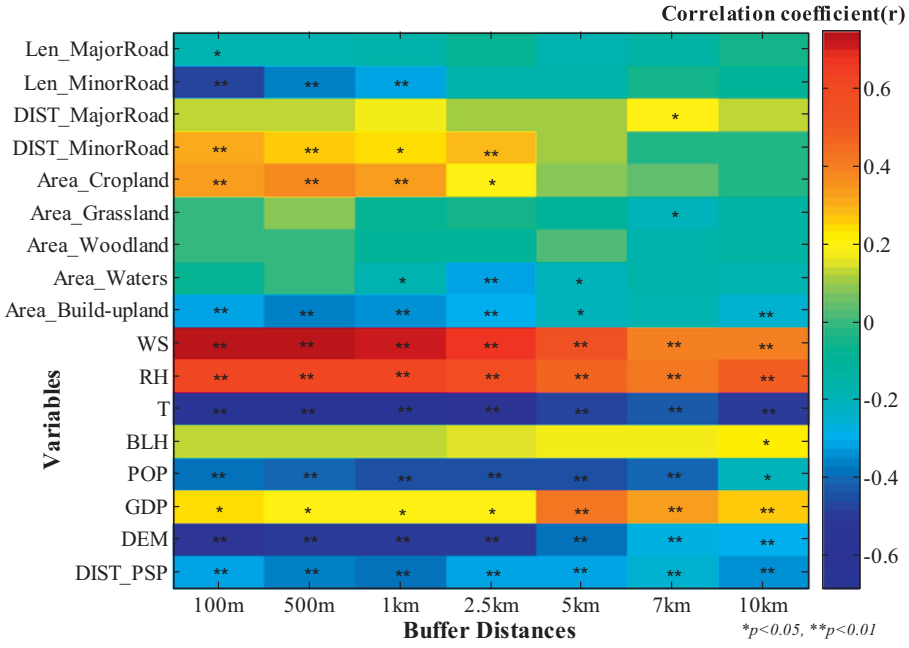

Fig. 7. Correlation coefficients (r) between MBC concentrations and potential predictor variables in 7 buffer distances.

Table 3
LUR model of BC (μg/m^3), including selected variables and results of LOOCV.

Independent variables	Regression coefficients	Model performance	LOOCV
Intercept	2.32	$R^2 = 0.68$	$R^2 = 0.66$
WS.100 m	0.10	Adjusted $R^2 = 0.67$	RMSE = 0.19
RH.100 m	0.15	RMSE = 0.19	
GDP.5 km	0.09		
DIST_PSP.1 km	−0.04		

(2015) developed LUR models for BC, and the adjusted R^2 was 0.35–0.40. Hankey and Marshall (2015a, 2015b) also established LUR model with mobile BC observations in Minneapolis, and their R^2 was 0.35. In addition, R^2 of LUR model for BC concentrations in Kerckhoffs et al. (2016) and Lee et al. (2017) were 0.12–0.30 and 0.50, respectively. This possible explanation was that the meteorological variables were considered in modeling in our study. We tried to exclude all meteorological variables in LUR modeling and found that the model would lose explanatory power, with R^2 decreased to 0.57. It might indicate that meteorology could cause a significant improvement in LUR models (Dons et al., 2013). While the adjusted R^2 of LUR models for BC reported by Saraswat et al. (2013) were 0.69–0.86 and higher than our results, it maybe because that Saraswat et al. (2013) took BC concentration of a background site into consideration during their LUR modeling. In Minet et al. (2017), they did not contain the fixed monitoring stations and thought that even the 'background' station of the air quality surveillance network has lately seen a large land-use development around it. For these reasons, we think LUR modeling for air pollution could also be feasible without the background BC values in this study.

It was important to note that road variables were not selected as independent variables and no "traffic" factor being accounted in the LUR model application. It was mainly due to the fact that the actual traffic conditions could not be reflected by road variables. Because of the vehicle ban regulation, the same road length and density may have different vehicle populations. In addition, due to the deficiency of traffic factors during LUR modeling, the simulation performance of LUR was limited. LUR modeling from mobile BC measurements was possible, but more work could usefully inform best practice, especially with the addition of traffic variables related to the actual traffic conditions and the different vehicle population (i.e. high emitting vehicles, relative clean vehicles).

With the established LUR model, we could map the BC in the urban traffic environment at a high spatial resolution (100 m) (Fig. 8). Due to the attributions of meteorological variables, i.e. WS.100 m and RH.100 m, the spatial distribution of exposure to BC in Shanghai showed a smooth and spatial continuity. The region with high BC concentrations (>10.88 μg/m^3) was mainly distributed in the northwestern and southeast regions, while the areas within the inner city appeared obviously lower exposure to BC in traffic environment. Besides, suburban districts in the southwest (e.g. Minhang, Songjiang) also performed a lower concentration level of BC exposure. The spatial distribution characteristic of atmospheric BC in traffic environment in Shanghai was also affected by the Shanghai traffic restriction policy. The northwestern and southeast areas of Shanghai were the main hub regions where heavy-polluting vehicles from other provinces entered Shanghai, where the container cars and diesel-fueled heavy trucks were the most representatives.

In the end, we tested the LUR model residuals using Moran's I to assess model performance. Moran's I of the residuals for the LUR model was 0.75, indicating a high spatial autocorrelation. The calculated result of the Moran's I in this study was close to those of Hankey and Marshall (2015a, 2015b), which ranged from 0.53–0.61 at 100 m search radius. To further explore the local spatial autocorrelation, we used the LISA analysis and mapped clusters of high values (model underestimates) and clusters of low values (model overestimates), shown in Fig. 8. Most residuals were not classified as clusters (model underestimates or overestimates) or outliers (including the two situations of low value near cluster of high values and high value near cluster of low values). The proportions of model underestimates and overestimates were 6.90% and 3.45%, respectively. Specifically, the model tended to underestimate BC concentrations in areas with high levels of congestion occurred (Hankey and Marshall, 2015a, 2015b).

3.4. Uncertainty in BC modeling with LUR model

The applicability of the LUR models in BC modeling is restricted by the characteristics of the input data (Van den Bossche et al., 2018). The most controversial aspect of mobile monitoring was that it cannot simultaneously consider the time synchronization when acquiring the observations at a high spatial resolution. Atmospheric pollutants are not only highly heterogeneous at spatially but also at small time scales (Van den Bossche et al., 2015). In our study, we used a round-trip sampling method for each route and repeated the monitoring several times, it may still not completely eliminate the time difference of observations. Due to the influences from traffic environment, such as traffic density and conditions, the observed BC concentrations in this study were inevitable suffered from uncertainty. To be specific, in this study, the total difference between inbound and outbound trip was 0.26 μg/m^3, with a relative deviation of 2.4%. For the repeatability of the three round-trip measurement, the relative deviation was 5.2%–7.6%. The sampling measurement with more repetition would helpful for making results more objective and decrease the uncertainty in LUR modeling.

The quality of the potential predictor variables and their representativeness would directly influence the model performance. In our study, traffic roads were obtained from open sources which may differ from the actual road distribution in Shanghai. In addition, road variables were not selected as independent variables in this study, which could limit the model performance. If the variables reflecting the population of high emitting vehicles could be considered in the LUR model, the model performance would be improved. Meanwhile, a rough land use classification might ignore the effect of a specific land use on BC concentration. In the studies illustrated in Hankey and Marshall (2015a, 2015b), the type of open space land and the land type of retail affect the spatial distribution of BC concentration.

The basic principle of the LUR model was based on the multiple linear regression analysis between the BC concentration and the influencing factors. However, atmospheric pollutants, including BC, were affected by many factors. Although there was no significant linear relationship between BC and environmental variables, there may be a certain non-linear relationship. He and Lin (2017) found that there was a linear $PM_{2.5}$ and wind speed, but there was a non-linear relationship between CO and O_3 and meteorological variables (i.e. precipitation, humidity). Therefore, it was possible to eliminate some non-linear related variables with LUR modeling, thereby increased the uncertainty of the model results. However, it cannot be denied that mobile monitoring and LUR model offered an alternative way in favor of obtaining data at a high spatial resolution and mapping the spatial distribution of air pollutant.

4. Conclusions

In this study, mobile measurements of urban BC exposure in traffic from three sampling routes covering 116 km were conducted during 9:00–11:00 am in Shanghai, the commercial and financial center in mainland China. The high spatial resolution of BC samplings could provide the opportunity to understand the urban BC in traffic environment and investigate its determinants. The average daytime (9:00–11:00 am) BC concentrations along these three transects in Shanghai was 10.77 ± 3.50 μg/m^3 in October and December 2016. The high BC value presented serious public health issues to the local population. BC concentrations in Shanghai showed a significant spatial heterogeneity, with the highest value appearing in the southeast followed by northwest and the lowest concentration appearing in the southwest region. It was worth nothing that the average BC in the low-degree urbanization areas (L_urban)

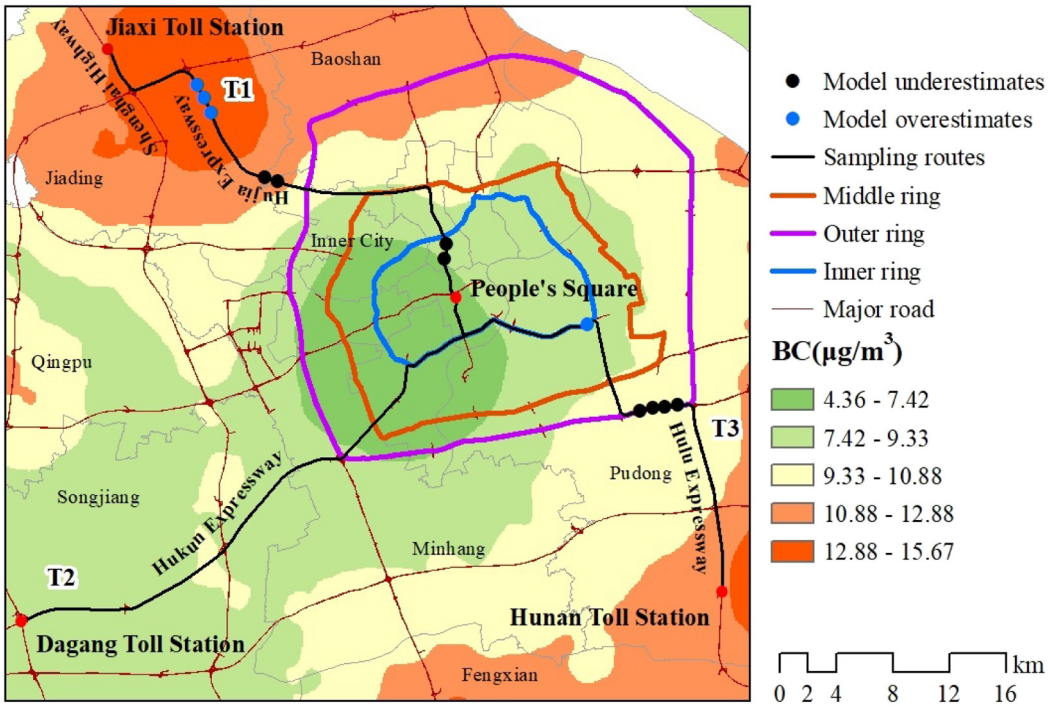

Fig. 8. The spatial variation of BC concentrations in Shanghai with LUR model.

were 57% higher (5.03 μg/m^3) than that in urban core (H_urban), which exhibited a well-shaped BC hole. This result implied that the trend of in-traffic BC in urban areas of Shanghai was likely to depend more on the traffic policy, such as the permission of diesel-fueled vehicles, and the distribution of high smoke and dust industrial emissions. Overall, an established LUR model in this study with seven geographic predictor variables could explain a proportion (68%) of the variability in measured BC concentration.

This study mainly focused on the spatial distribution and its determinants of in-traffic BC concentrations in urban areas. The BC measurements obtained from mobile sampling campaign were assumed to be representative at the regional level. As the high spatiotemporal heterogeneity of BC concentrations in urban area, the BC measurements with mobile platform were inevitable suffered from uncertainty, which also lead to the uncertainty in LUR modeling. The quantification of different BC sources on reginal BC concentrations in urban area still need further clarification, especially the actual effect of traffic regulation policy. Additional studies on urban BC concentrations in different parts of the city with different sampling methods and long-term measuring are also needed.

Acknowledgements

This work jointly supported by the National Key Research and Development Program (2017YFC0500204, 2016YFC0500204), the Natural Science Foundation of Shanghai (17ZR1408700), Shanghai Technology innovation action plan of Yangtze River Delta joint research projects (17295810603), National Natural Science Foundation of China (41471076), and Key Laboratory of Spatial Data Mining & Information Sharing of Ministry of Education, Fuzhou University (No. 2017LSDMIS07). We would like to thank Dr. Varenyam Achal for proofreading our revised manuscript.

References

Apte, J.S., Kirchstetter, T.W., Reich, A.H., Deshpande, S.J., Kaushik, G., Chel, A., Marshall, J.D., Nazaroff, W.W., 2011. Concentrations of fine, ultrafine, and black carbon particles in auto-rickshaws in New Delhi, India. Atmos. Environ. 45, 4470–4480. https://doi.org/10.1016/j.atmosenv.2011.05.028.

Bahadur, R., Feng, Y., Russell, L.M., Ramanathan, V., 2011. Impact of California's air pollution laws on black carbon and their implications for direct radiative forcing. Atmos. Environ. 45, 1162–1167. https://doi.org/10.1016/j.atmosenv.2010.10.054.

Begam, G.R., Vachaspati, C.V., Ahammed, Y.N., Kumar, K.R., Babu, S.S., Reddy, R.R., 2016. Measurement and analysis of black carbon aerosols over a tropical semi-arid station in Kadapa, India. Atmos. Res. 171, 77–91. https://doi.org/10.1016/j.atmosres.2015.12.014.

Booth, B., Bellouin, N., 2015. Climate change: black carbon and atmospheric feedbacks. Nature 519, 167–168. https://doi.org/10.1038/519167a.

Cape, J.N., Coyle, M., Dumitrean, P., 2012. The atmospheric lifetime of black carbon. Atmos. Environ. 59, 256–263. https://doi.org/10.1016/j.atmosenv.2012.05.030.

Chan, C.K., Yao, X., 2008. Air pollution in mega cities in China. Atmos. Environ. 42, 1–42. https://doi.org/10.1016/j.atmosenv.2007.09.003.

Chen, J., Chen, J., Liao, A.P., Cao, X., Chen, L.J., Chen, X.H., He, C.Y., Han, G., Peng, S., Lu, M., Zhang, W.W., Tong, X.H., Mills, J., 2015. Global land cover mapping at 30 m resolution: a POK-based operational approach. ISPRS J. Photogramm. Remote Sens. 103, 7–27. https://doi.org/10.3390/ijgi5110217.

Cheng, Y.H., Lin, M.H., 2013. Real-time performance of the microAeth (R) AE51 and the effects of aerosol loading on its measurement results at a traffic site. Aerosol Air Qual. Res. 13, 1853–1863. https://doi.org/10.4209/aaqr.2012.12.0371.

Dabass, A., Talbott, E.O., Venkat, A., Rager, J., Marsh, G.M., Sharma, R.K., Holguin, F., 2016. Association of exposure to particulate matter (PM2.5) air pollution and biomarkers of cardiovascular disease risk in adult NHANES participants (2001–2008). Int. J. Hyg. Environ. Health 219, 301–310. https://doi.org/10.1016/j.ijheh.2015.12.002.

Dekoninck, L., Botteldooren, D., Int Panis, L., Hankey, S., Jain, G., Karthik, S., Marshall, J., 2015. Applicability of a noise-based model to estimate in-traffic exposure to black carbon and particle number concentrations in different cultures. Environ. Int. 74, 89–98. https://doi.org/10.1016/j.envint.2014.10.002.

Ding, A.J., Huang, X., Nie, W., Sun, J.N., Kerminen, V.M., Petaja, T., Su, H., Cheng, Y.F., Yang, X.Q., Wang, M.H., Chi, X.G., Wang, J.P., Virkkula, A., Guo, W.D., Yuan, J., Wang, S.Y., Zhang, R.J., Wu, Y.F., Song, Y., Zhu, T., Zilitinkevich, S., Kulmala, M., Fu, C.B., 2016. Enhanced haze pollution by black carbon in megacities in China. Geophys. Res. Lett. 43, 2873–2879. https://doi.org/10.1002/2016GL067745.

Dons, E., Van Poppel, M., Kochan, B., Wets, G., Int Panis, L., 2013. Modeling temporal and spatial variability of traffic-related air pollution: hourly land use regression models for black carbon. Atmos. Environ. 74, 237–246. https://doi.org/10.1016/j.atmosenv.2013.03.050.

Dumka, U.C., Manchanda, R.K., Sinha, P.R., Sreenivasan, S., Moorthy, K.K., Babu, S.S., 2013. Temporal variability and radiative impact of black carbon aerosol over tropical urban station Hyderabad. J. Atmos. Sol. Terr. Phys. 105, 81–90. https://doi.org/10.1016/j.jastp.2013.08.003.

Geng, F.H., Hua, J., Mu, Z., Peng, L., Xu, X.H., Chen, R.J., Kan, H.D., 2013. Differentiating the associations of black carbon and fine particle with daily mortality in a Chinese city. Environ. Res. 120, 27–32. https://doi.org/10.1016/j.envres.2012.08.007.

Grieshop, A.P., Reynolds, C.C.O., Kandlikar, M., Dowlatabadi, H., 2009. A black-carbon mitigation wedge. Nat. Geosci. 2, 533–534. https://doi.org/10.1038/ngeo595.

Grimm, N.B., Faeth, S.H., Golubiewski, N.E., Redman, C.L., Wu, J.G., Bai, X.M., Briggs, J.M., 2008. Global change and the ecology of cities. Science 319, 756–760. https://doi.org/10.1126/science.1150195.

Hagler, G.S.W., Yelverton, T.L.B., Vedantham, R., Hansen, A.D.A., Turner, J.R., 2011. Post-processing method to reduce noise while preserving high time resolution in

aethalometer real-time black carbon data. Aerosol Air Qual. Res. 11, 539–546. https://doi.org/10.4209/aaqr.2011.05.0055.
Hankey, S., Marshall, J.D., 2015a. On-bicycle exposure to particulate air pollution: particle number, black carbon, PM2.5, and particle size. Atmos. Environ. 122, 65–73. https://doi.org/10.1016/j.atmosenv.2015.09.025.
Hankey, S., Marshall, J.D., 2015b. Land use regression models of on-road particulate air pollution (particle number, black carbon, PM2.5, particle size) using mobile monitoring. Environ. Sci. Technol. 49, 9194–9202. https://doi.org/10.1021/acs.est.5b01209.
Hansen, J., Sato, M., Ruedy, R., Lacis, A., Oinas, V., 2000. Global warming in the twenty-first century: an alternative scenario. Proc. Natl. Acad. Sci. U. S. A. 97, 9875–9880. https://doi.org/10.1073/pnas.170278997.
Hansen, A.D.A., Lowenthal, D.H., Chow, J.C., Watson, J.G., 2001. Black carbon aerosol at McMurdo station, Antarctica. J. Air Waste Manage. Assoc. 51, 593–600. https://doi.org/10.1080/10473289.2001.10464283.
Harrison, R.G., 2006. Urban smoke concentrations at Kew, London, 1898–2004. Atmos. Environ. 40, 3327–3332. https://doi.org/10.1016/j.atmosenv.2006.01.042.
He, X., Lin, Z., 2017. Interactive effects of the influencing factors on the changes of PM2.5 concentration based on GAM model. Environ. Sci. 38, 22–32. https://doi.org/10.13227/j.hjkx.201606061 (in Chinese).
Highwood, E.J., Kinnersley, R.P., 2006. When smoke gets in our eyes: the multiple impacts of atmospheric black carbon on climate, air quality and health. Environ. Int. 32, 560–566. https://doi.org/10.1016/j.envint.2005.12.003.
Invernizzi, G., Ruprecht, A., Mazza, R., De Marco, C., Mocnik, G., Sioutas, C., Westerdahl, D., 2011. Measurement of black carbon concentration as an indicator of air quality benefits of traffic restriction policies within the ecopass zone in Milan, Italy. Atmos. Environ. 45, 3522–3527. https://doi.org/10.1016/j.atmosenv.2011.04.008.
IPCC, 2001. Climate change 2001: Impacts, adaptation, and vulnerability. Contribution of Working Group II to the Third Assessment Report of the Intergovernmental Panel on Climate Change. Cambridge University Press, New York, NY.
IPCC, 2013. Climate change 2013: the physical science basis. In: Stocker, T.F., Qin, D., Plattner, G.K., Tignor, M., et al. (Eds.), Contribution of Working Group I to the Fifth Assessment Report of the Intergovernmental Panel on Climate Change. Cambridge University Press, New York, NY.
Janssen, N.A.H., Hoek, G., Simic-Lawson, M., Fischer, P., van Bree, L., ten Brink, H., Keuken, M., Atkinson, R.W., Anderson, H.R., Brunekreef, B., Cassee, F.R., 2011. Black carbon as an additional Indicator of the adverse health effects of airborne particles compared with PM10 and PM2.5. Environ. Health Perspect. 119, 1691–1699. https://doi.org/10.1289/ehp.1003369.
Kerckhoffs, J., Hoek, G., Messier, K.P., Brunekreef, B., Meliefste, K., Klompmaker, J.O., Vermeulen, R., 2016. Comparison of ultrafine particle and black carbon concentration predictions from a mobile and short-term stationary land-use regression model. Environ. Sci. Technol. 50, 12894–12902. https://doi.org/10.1021/acs.est.6b03476.
Kim, S., Yu, S., Yun, D., 2017. Spatiotemporal association of real-time concentrations of black carbon (BC) with fine particulate matters (PM2.5) in urban hotspots of South Korea. Int. J. Environ. Res. Public Health 14, 1350. https://doi.org/10.3390/ijerph14111350.
Kirchstetter, T.W., Novakov, T., 2007. Controlled generation of black carbon particles from a diffusion flame and applications in evaluating black carbon measurement methods. Atmos. Environ. 41, 1874–1888. https://doi.org/10.1016/j.atmosenv.2006.10.067.
Kirchstetter, T.W., Aguiar, J., Tonse, S., Fairley, D., Novakov, T., 2008. Black carbon concentrations and diesel vehicle emission factors derived from coefficient of haze measurements in California: 1967–2003. Atmos. Environ. 42, 480–491. https://doi.org/10.1016/j.atmosenv.2007.09.063.
Kirchstetter, T.W., Preble, C.V., Hadley, O.L., Bond, T.C., Apte, J.S., 2017. Large reductions in urban black carbon concentrations in the United States between 1965 and 2000. Atmos. Environ. 151, 17–23. https://doi.org/10.1016/j.atmosenv.2016.11.001.
Laborde, M., Crippa, M., Tritscher, T., Juranyi, Z., Decarlo, P.F., Temime-Roussel, B., Marchand, N., Eckhardt, S., Stohl, A., Baltensperger, U., Prevot, A.S.H., Weingartner, E., Gysel, M., 2013. Black carbon physical properties and mixing state in the European megacity Paris. Atmos. Chem. Phys. 13, 5831–5856. https://doi.org/10.5194/acp-13-5831-2013.
Latha, K.M., Badarinath, K.V., 2004. Correlation between black carbon aerosols, carbon monoxide and tropospheric ozone over a tropical urban site. Atmos. Res. 71, 265–274. https://doi.org/10.1016/j.atmosres.2004.06.004.
Lee, M., Brauer, M., Wong, P.L.N., Tang, R., Tsui, T.H., Choi, C., Cheng, W., Lai, P.C., Tian, L.W., Thach, T.Q., Allen, R., Barratt, B., 2017. Land use regression modelling of air pollution in high density high rise cities: a case study in Hong Kong. Sci. Total Environ. 592, 306–315. https://doi.org/10.1016/j.scitotenv.2017.03.094.
Lei, X.N., Bian, J.W., Xiu, G.L., Hu, X.F., Gu, X.S., Bian, Q.G., 2017. The mobile monitoring of black carbon and its association with roadside data in the Chinese megacity of Shanghai. Environ. Sci. Pollut. Res. Int. 24, 7482–7489. https://doi.org/10.1007/s11356-017-8454-2.
Leventidou, E., Zanis, P., Balis, D., Giannakaki, E., Pytharoulis, I., Amiridis, V., 2013. Factors affecting the comparisons of planetary boundary layer height retrievals from CALIPSO, ECMWF and radiosondes over Thessaloniki, Greece. Atmos. Environ. 74, 360–366.
Li, B., Lei, X.N., Xiu, G.L., Gao, C.Y., Gao, S., Qian, N.S., 2015. Personal exposure to black carbon during commuting in peak and off-peak hours in Shanghai. Sci. Total Environ. 524, 237–245. https://doi.org/10.1016/j.scitotenv.2015.03.088.
Liu, D., Flynn, M., Gysel, M., Targino, A., Crawford, I., Bower, K., Choularton, T., Juranyi, Z., Steinbacher, M., Huglin, C., Curtius, J., Kampus, M., Petzold, A., Weingartner, E., Baltensperger, U., Coe, H., 2010. Single particle characterization of black carbon aerosols at a tropospheric alpine site in Switzerland. Atmos. Chem. Phys. 10, 7389–7407. https://doi.org/10.5194/acp-10-7389-2010.
Menon, S., Hansen, J., Nazarenko, L., Luo, Y.F., 2002. Climate effects of black carbon aerosols in China and India. Science 297, 2250–2253. https://doi.org/10.1126/science.1075159.
Minet, L., Gehr, R., Hatzopoulou, M., 2017. Capturing the sensitivity of land-use regression models to short-term mobile monitoring campaigns using air pollution microsensors. Environ. Pollut. 230, 280–290. https://doi.org/10.1016/j.envpol.2017.06.071.
Moloi, K., Chimidza, S., Lindgren, E.S., Viksna, A., Standzenieks, P., 2002. Black carbon, mass and elemental measurements of airborne particles in the village of Serowe, Botswana. Atmos. Environ. 36, 2447–2457. https://doi.org/10.1016/S1352-2310(02)00085-7.
Montagne, D.R., Hoek, G., Klompmaker, J.O., Wang, M., Meliefste, K., Brunekreef, B., 2015. Land use regression models for ultrafine particles and black carbon based on short-term monitoring predict past spatial variation. Environ. Sci. Technol. 49, 8712–8720. https://doi.org/10.1021/es505791g.
Mooney, P., Minghini, M., Laakso, M., Antoniou, V., Olteanu-Raimond, A.M., Skopeliti, A., 2016. Towards a protocol for the collection of VGI vector data. ISPRS Int. J. Geo-Inf. 5.
Morales Betancourt, R., Galvis, B., Balachandran, S., Romos-Bonilla, J.P., Sarmiento, O.L., Gallo-Murcia, S.M., Contreras, Y., 2017. Exposure to fine particulate, black carbon, and particle number concentration in transportation microenvironments. Atmos. Environ. 157, 135–145. https://doi.org/10.1016/j.atmosenv.2017.03.006.
Murphy, D.M., Chow, J.C., Leibensperger, E.M., Malm, W.C., Pitchford, M., Schichtel, B.A., Watson, J.G., White, W.H., 2011. Decreases in elemental carbon and fine particle mass in the United States. Atmos. Chem. Phys. 11, 4679–4686. https://doi.org/10.5194/acp-11-4679-2011.
Ni, M.J., Huang, J.X., Lu, S.Y., Li, X.D., Yan, J.H., Cen, K.F., 2014. A review on black carbon emissions, worldwide and in China. Chemosphere 107, 83–93. https://doi.org/10.1016/j.chemosphere.2014.02.052.
Nordbo, A., Jarvi, L., Haapanala, S., Wood, C.R., Vesala, T., 2012. Fraction of natural area as main predictor of net CO_2 emissions from cities. Geophys. Res. Lett. 39 (20). https://doi.org/10.1029/2012GL053087.
Nunen, E.V., Vermeulen, R., Tsai, M.Y., Probsthensch, N., Ineichen, A., Davey, M.E., Imboden, M., Ducret-Stich, R., Naccarati, A., Raffaele, D., Ranzi, A., Ivaldi, C., Galassi, C., Nieuwenhuijsen, M., Curto, A., Donaire-Gonzalez, D., Cirach, M., Chatzi, L., Kampouri, M., Vlaanderen, J., Meliefste, K., Buijtenhuijs, D., Brunekreef, B., Morley, D., Vineis, P., Gulliver, J., Hoek, G., 2017. Land use regression models for ultrafine particles in six European areas. Environ. Sci. Technol. 51, 3336–3345. https://doi.org/10.1021/acs.est.6b05920.
Qin, Y., Xie, S.D., 2012. Spatial and temporal variation of anthropogenic black carbon emissions in China for the period 1980–2009. Atmos. Chem. Phys. 12, 4825–4841. https://doi.org/10.5194/acp-12-4825-2012.
Rajesh, T.A., Ramachandran, S., 2017. Characteristics and source apportionment of black carbon aerosols over an urban site. Environ. Sci. Pollut. Res. Int. 24, 8411–8424. https://doi.org/10.1007/s11356-017-8453-3.
Ramanathan, V., Carmichael, G., 2008. Global and regional climate changes due to black carbon. Nat. Geosci. 1, 221–227. https://doi.org/10.1038/ngeo156.
Rattigan, O.V., Civerolo, K., Doraiswamy, P., Felton, H.D., Hopke, P.K., 2013. Long term black carbon measurements at two urban locations in New York. Aerosol Air Qual. Res. 13, 1181–U1305. https://doi.org/10.4209/aaqr.2013.02.0060.
Safai, P.D., Raju, M.P., Budhavant, K.B., Rao, P.S.P., Devara, P.C.S., 2013. Long term studies on characteristics of black carbon aerosols over a tropical urban station Pune, India. Atmos. Res. 132, 173–184. https://doi.org/10.1016/j.atmosres.2013.05.002.
Saraswat, A., Apte, J.S., Kandlikar, M., Brauer, M., Henderson, S.B., Marshall, J.D., 2013. Spatiotemporal land use regression models of fine, ultrafine, and black carbon particulate matter in New Delhi, India. Environ. Sci. Technol. 47, 12903–12911. https://doi.org/10.1021/es401489h.
Shanghai Statistics Bureau, 2017. Shanghai Statistical Yearbook. China Statistics Press, Beijing.
Tan, H.B., Liu, L., Fan, S.J., Li, F., Yin, Y., Cai, M.F., Chan, P.W., 2016. Aerosol optical properties and mixing state of black carbon in the Pearl River Delta, China. Atmos. Environ. 131, 196–208. https://doi.org/10.1016/j.atmosenv.2016.02.003.
Targino, A.C., Gibson, M.D., Krecl, P., Rodrigues, M.V.C., dos Santos, M.M., Correa, M.D., 2016. Hotspots of black carbon and PM2.5 in an urban area and relationships to traffic characteristics. Environ. Pollut. 218, 475–486. https://doi.org/10.1016/j.envpol.2016.07.027.
Van den Bossche, J., Peters, J., Verwaeren, J., Botteldooren, D., Theunis, J., De Baets, B., 2015. Mobile monitoring for mapping spatial variation in urban air quality: development and validation of a methodology based on an extensive dataset. Atmos. Environ. 105, 148–161. https://doi.org/10.1016/j.atmosenv.2015.01.017.
Van den Bossche, J., De Baets, B., Verwaeren, J., Botteldooren, D., Theunis, J., 2018. Development and evaluation of land use regression models for black carbon based on bicycle and pedestrian measurements in the urban environment. Environ. Model. Softw. 99, 58–69. https://doi.org/10.1016/j.envsoft.2017.09.019.
Vinogradova, A.A., Fedorova, E.I., Belikov, I.B., Ginzburg, A.S., Elansky, N.F., Skorokhod, A.I., 2007. Temporal variations in carbon dioxide and methane concentrations under urban conditions. Izv. Atmos. Oceanic Phys. 43, 599–611.
Vilcassim, M.J.R., Thurston, G.D., Peltier, R.E., Gordon, T., 2014. Black carbon and particulate matter (PM2.5) concentrations in New York City's subway stations. Environ. Sci. Technol. 48, 14738–14745. https://doi.org/10.1021/es504295h.
Wang, X., Westerdahl, D., Wu, Y., Pan, X.C., Zhang, K.M., 2011. On-road emission factor distributions of individual diesel vehicles in and around Beijing, China. Atmos. Environ. 45, 503–513. https://doi.org/10.1016/j.atmosenv.2010.09.014.
Winiger, P., Andersson, A., Eckhardt, S., Stohl, A., Semiletov, I.P., Dudarev, O.V., Charkin, A., Shakhova, N., Klimont, Z., Heyes, C., Gustafsson, Ö., 2017. Siberian Arctic black carbon sources constrained by model and observation. Proc. Natl. Acad. Sci. U. S. A. 114, 1054–1061. https://doi.org/10.1073/pnas.1613401114.
WMO/GAW, 2003. WMO/GAW Aerosol Measurement Procedures Guidelines and Recommendations. World Meteorological Organization, Geneva.
Zhang, X.L., Rao, R.Z., Huang, Y.B., Mao, M., Berg, M.J., Sun, W.B., 2015. Black carbon aerosols in urban central China. J. Quant. Spectrosc. Radiat. Transf. 150, 3–11. https://doi.org/10.1016/j.jqsrt.2014.03.006.